McKinsey & Company

Technical appendix

Valuing nature conservation: A methodology for quantifying the benefits of protecting the planet's natural capital

In this appendix, we detail the approach we used to estimate some of the costs and benefits of expanding nature conservation. The approach was designed and performed by McKinsey & Company's agricultural and environmental advanced-analytics center (ACRE), which built on peer-reviewed methodologies and existing data points or spatial data layers. Our analytics have a global scope. Considering the necessary simplification, as well as the potential inaccuracies of the data at such a large scale, the results are not intended to represent precise local geographic contexts or recent local developments (political or otherwise). Although our analytics can provide useful directional guidance, drawing any local conclusions will require additional detailed, local studies.

Geographic divisions of the Earth's surface

Our analysis uses different divisions of the Earth's surface.

First are ecozones (also known as biogeographic realms), of which there are eight on land, according to Olson et al.,[1] and 12 in coastal and shelf areas, according to the classification of Spalding et al.[2] Each represents a large region with distinct distributional patterns of organisms as a result of long-lasting isolating features such as oceans, broad deserts, or mountains on land, or water temperature and the proximity of benthos in oceans. These ecozones are shown in Exhibit 1.

There are 14 terrestrial biomes, each representing a collection of plants and animals formed under similar climate conditions. Biomes can span continents and are shown in Exhibit 2.[3]

Nested within the ecozones and biomes are ecoregions, of which there are 867 on land and 232 in coastal and shelf areas. Each ecoregion represents a unit of land or water that contains a distinct assemblage of natural communities and species that evolve under similar environmental conditions (such as climate, geology, and water resources). These ecoregions are shown in Exhibit 3.

Analysis of existing protected areas[3]

We estimated the potential benefits and costs of nature conservation in two types of areas:

1. currently unprotected areas identified for potential conservation, termed here as new conservation areas (NCAs)

2. existing protected areas (PAs[4]) experiencing high-potential risks from human pressures (abbreviated here as PAs at risk, or PARs)

Terrestrial PARs were identified via the use of the Human Footprint (HFP) index, which represents an aggregated measure of human pressure on the environment. The index considers eight metrics that are linked to human activities: built environments, intensive agriculture, pasture lands, human population density, night-time lights, roads, railways, and navigable waterways. The resulting score ranges from 0 (no human activity) to 50, with a score below 4 indicating lands predominantly free of permanent infrastructure; HFP data have a spatial resolution of one square kilometer and cover a time window of 16 years (1993–2009).

[1] D. M. Olson et al., "Terrestrial ecoregions of the world: A new map of life on Earth," "it al Bioscience", 2001, Volume 51, number 11, pp. 933–8.
[2] M. D. Spalding et al., "Marine ecoregions of the world: A bioregionalization of coastal and shelf areas," BioScience, July 2007, Volume 57, Number 11, "it al BioScience", pp. 573–83.
[3] Inland water, and rock and ice are not considered biomes.
[4] Protected Areas as defined under International Union for Conservation of Nature categories were considered in the analysis of existing conservation areas. Other effective conservation measures (OECMs) were not considered, given a lack of sufficiently robust, detailed, and exhaustive spatially explicit data. In this analysis, new conservation areas that result in 30 percent global conservation are assumed to comprise both OECMs and PAs.

Exhibit 1

There are eight terrestrial ecozones (also known as biogeographic realms, top) and 12 marine ecozones (bottom).

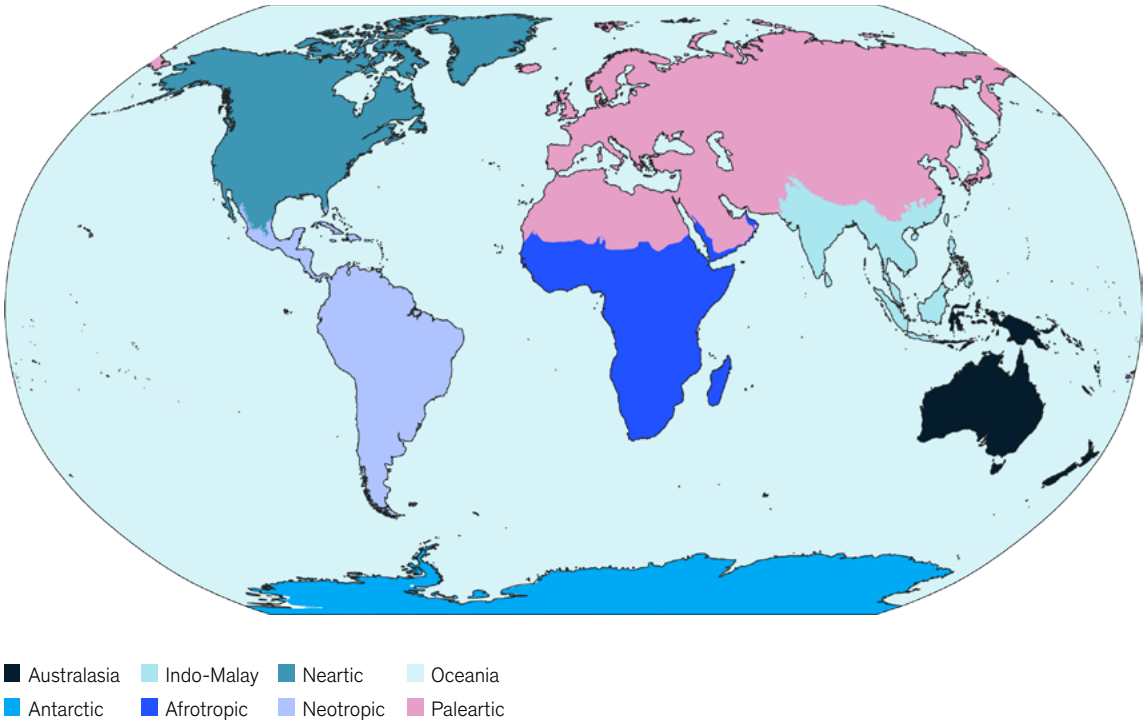

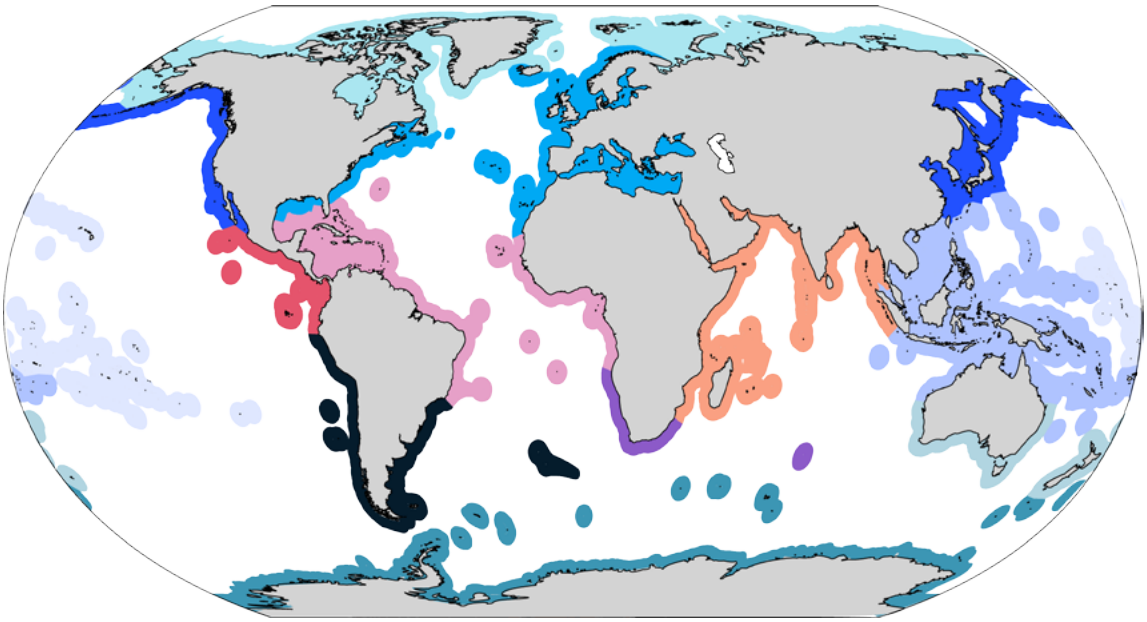

Source: D. M. Olson et al., "Terrestrial ecoregions of the world: A new map of life on Earth," BioScience, Volume 51, Number 11, pp. 933–8 and The Nature Conservancy. M. D. Spalding et al., "Marine ecoregions of the world: A bioregionalization of coastal and shelf areas," ***BioScience***, July 2007, Volume 57, Number 11, pp. 573–83.

Exhibit 2

There are 14 terrestrial biomes.

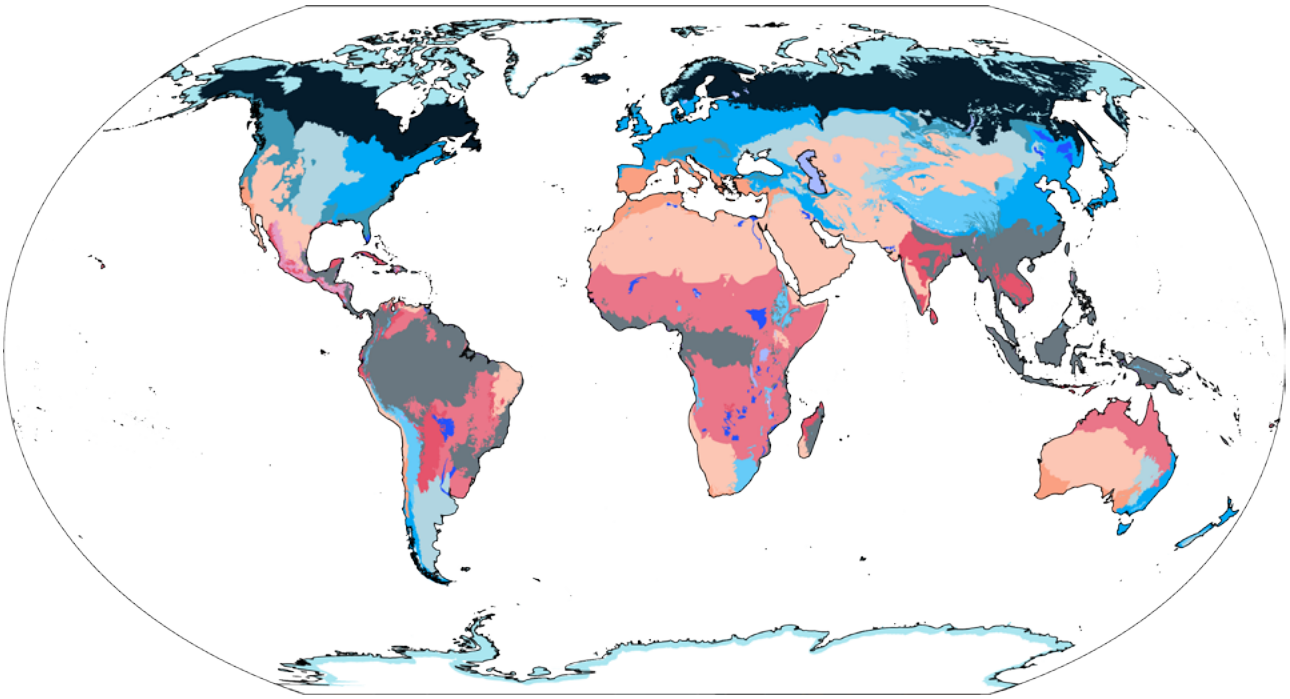

- Boreal forests/taiga
- Deserts and xeric shrublands
- Flooded grasslands and savannas
- Inland water
- Mangroves
- Mediterranean forests, woodlands, and scrub
- Montane grasslands and shrublands
- Rock and ice
- Temperate broadleaf and mixed forests
- Temperate conifer forests
- Temperate grasslands, savannas, and shrublands
- Tropical and subtropical coniferous forests
- Tropical and subtropical dry broadleaf forests
- Tropical and subtropical grasslands, savannas, and shrublands
- Tropical and subtropical moist broadleaf forests
- Tundra

Source: D. M. Olson et al., BioScience, 2001, Volume 51, pp. 933–8 and The Nature Conservancy. M. D. Spalding et al., "Marine ecoregions of the world: A bioregionalization of coastal and shelf areas," BioScience, 2007, Volume 57, pp. 573–83.

A direct link between these pressures and declines in biodiversity has been demonstrated.[5] The rate of change in each existing PA during the period from 1993 to 2009 was computed as the mean difference between HFP values in 1993 and in 2009 within each PA, divided by the number of years (16), where negative values indicate a decrease in the HFP. For the approximately 35 percent of existing PAs established after 1993, we multiplied the rate of change of HFP observed in the ecoregion of the PA with the 1993 HFP value and the number of years separating the date the PA was established with 1993. A corrected rate of change was then computed using this value and the HFP in 2009. PAs created after 2009 (approximately 12 percent of existing PAs) were excluded from the analysis.

[5] M. Di Marco et al., "Changes in human footprint drive changes in species extinction risk," *Nature Communications*, November 2018, Volume 9, Article Number 4621, pp. 9, nature.com.

Exhibit 3

There are 867 terrestrial ecoregions and 232 marine ecoregions.

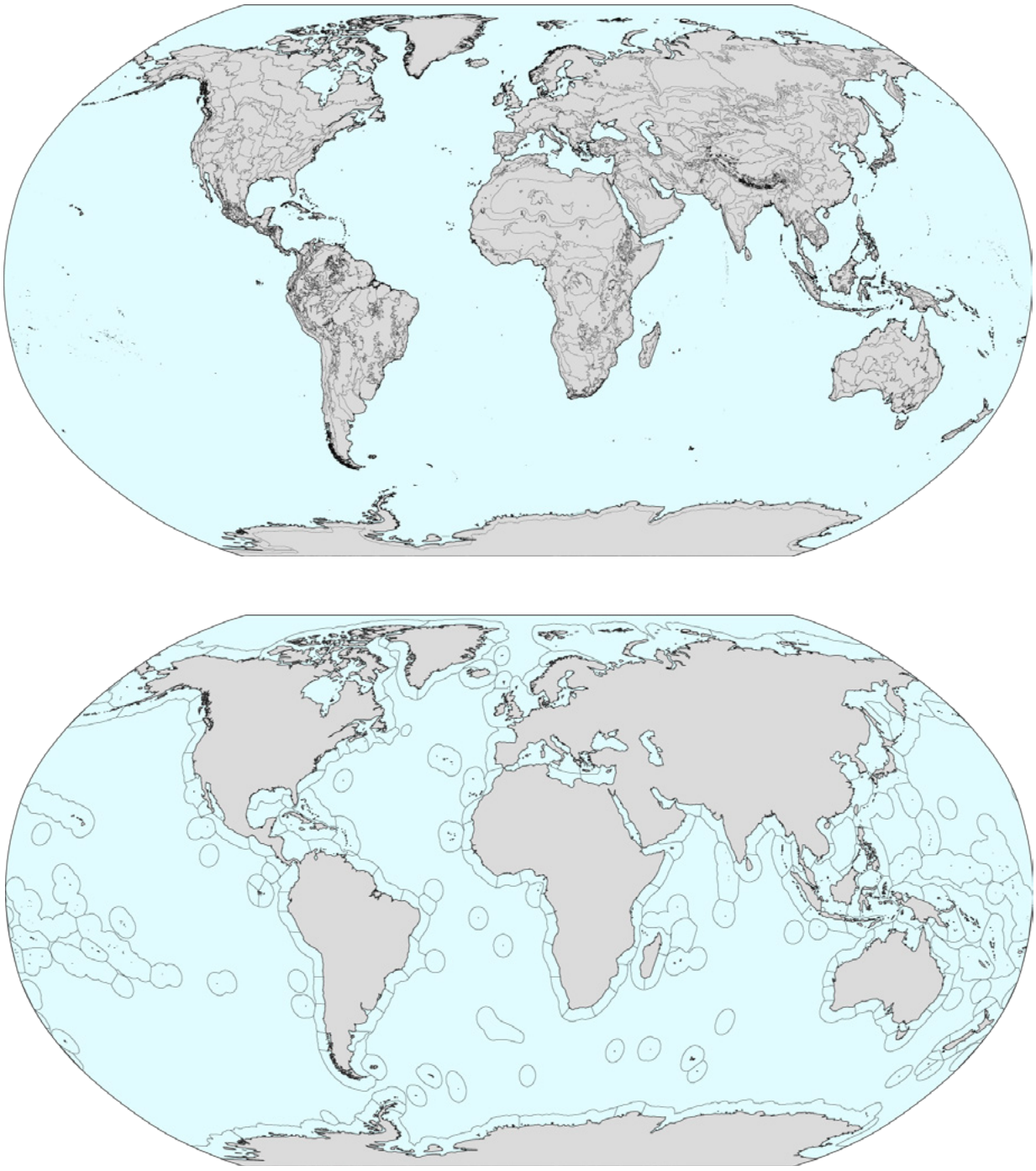

Source: D. M. Olson et al., "Terrestrial ecoregions of the world: A new map of life on Earth," BioScience, Volume 51, Number 11, pp. 933–8 and The Nature Conservancy. M. D. Spalding et al., "Marine ecoregions of the world: A bioregionalization of coastal and shelf areas," *BioScience*, July 2007, Volume 57, Number 11, pp. 573–83.

We created an index HPF_{diff} corresponding to the difference in a given PA between its HFP rate of change and the HFP mean rate of change of the ecoregion it belongs to. Values below zero indicated that the PA was less affected by increased human pressure compared to its ecoregion.

Different biases might have an impact on the HFP and hence the selection of potential PARs. For instance, the HFP tends to decrease with PA size, due to a dilution of human activities within large PAs and lower accessibility, since most human activities tend to occur on the fringes of PAs.[6] Furthermore, PAs characterized by a high level of remoteness, a high elevation, or a higher level of protection, according to their International Union for Conservation of Nature (IUCN) category, generally have a lower HFP index.

We established several HFP-derived metrics controlling for these biases. Briefly, we calculated the residuals (HFP_{resid}) of the linear regression between HFP and controlling factors and considered PARs as PAs with the following characteristics: $HFP_{2009} > 4$ (indicating human presence); $HFP_{diff} > 0$ (indicating a negative trend in human pressure compared to its ecoregion); and $HFP_{resid} > 0$ (indicating high HFP when controlling for its IUCN category, size, remoteness, and elevation).

Marine PARs were identified using an approach similar to that used for terrestrial PARs. The Cumulative Human Pressure (CHP) index is an aggregated measure of 14 human stressors on coastal areas and oceans, grouped in four categories: commercial and artisanal fishing, ocean-based (shipping), land-based (nutrient and organic chemical pollution, for example), and climate change (land-based acidification and sea surface temperature, for example). CHP data have a spatial resolution of 1 square kilometer and cover a time window of 10 years (2003–2013). A cumulative score, ranging from 0 (no pressure) to 5 (extreme pressure), is calculated via the summation of these stressors, with consideration of the vulnerability of each ecosystem to each stressor.

As with the approach used to detect terrestrial PARs, we created an index CHP_{diff} corresponding to the difference in a given PA between its CHP rate of change and the CHP mean rate of change of the marine ecoregion it belongs to, and we established several CHP-derived metrics controlling for CHP biases to properly identify PARs. We identified marine PARs as PA with (1) $CHP_{diff} > 0$, (2) $CHP_{2013} > 0.4$, and (3) $CHP_{resid} > 0$.

Identification of 30 percent of land and national waters to conserve

We obtained spatial data on the location of 214,921 PAs from the January 2020 version of the World Database on Protected Areas (WDPA).[7] We handled the WDPA data according to best-practice guidelines.[8] PAs represented as data points were converted to polygons using a geodesic buffer around the point based on its real attributes, excluding points with no attributes.

We used integer linear programming[9] to identify spatial priorities for meeting species-conservation targets while accounting for current conservation resulting from existing PAs ("locked-in" areas) and areas that cannot be conserved ("locked-out" areas such as cities) and minimizing the costs of

[6] See, for example, M. P. Veldhuis et al., "Cross-boundary human impacts compromise the Serengeti-Mara ecosystem," *Science,* March 29, 2019, Volume 363, Number 6434, pp. 1424–8, sciencemag.org.
[7] Protected Area data downloaded from the Integrated Biodiversity Assessment Tool (IBAT) (http://www.ibat-alliance.org). Provided by BirdLife International, Conservation International, IUCN, and UNEP-WCMC. Please contact ibat@ibat-alliance.org for further information.
[8] Available at https://www.protectedplanet.net/en/resources/calculating-protected-area-coverage.
[9] As implemented in Hanson JO, Schuster R, Morrell N, Strimas-Mackey M, Watts ME, Arcese P, Bennett J, Possingham HP (2020). prioritizr: Systematic Conservation Prioritization in R. R package version 5.0.3. Available at https://CRAN.R-project.org/package=prioritizr.

protection (the minimum-set problem). To run the analysis, we used a gridded image of the world across land and oceans from which pixels, also called planning units (PUs), are either selected or excluded to form a given solution of the conservation problem.

We used pixels of 5 × 5 kilometers for land and 30 × 30 kilometers for oceans. We calculated the area of each conservation feature (species distribution, for example) within each PU, including the area within existing PAs. For marine prioritization, we considered only national waters.[10] International waters were excluded, given the current challenges (for example, complex regulatory frameworks and management of multiple stakeholders) linked to the long-term protection of these areas. All geospatial data processing was carried out on a large cloud-computing machine.[11]

Prioritization was run separately for each ecozone to reduce computing time, assuming that it would only slightly affect the final solution in comparison to a global prioritization. This zonation also enables separate habitat protection of species with migratory trajectories between the different ecozones (for example, birds with a distribution range spanning two or more ecozones have relative protection targets set in each one of them).

Areas locked in, locked out

All existing PAs with "designated," "inscribed," or "established" status in the WDPA were "locked in," meaning they will be present in the set of conservation areas that are defined, no matter any given constraints, provided the solution is feasible. Since Chinese PAs are not included in the WDPA, we used a global layer of potential and likely critical habitats from Martin et al.,[12] which includes (among other areas) the missing Chinese PAs. We cropped the spatial layer to Chinese land and national waters and added them to the WDPA. To limit discrepancies between PA coverage when transferring polygons to PUs (for example, losing most PAs smaller than the grid size), we computed the coverage percentage of the PAs within each PU, sorted them from highest to lowest within each country and locked in PUs in descending order until reaching the relevant terrestrial or marine percentage PA coverage as reported by the Digital Observatory for Protected Areas.[13]

Major built-up areas and other areas with significant human activity were filtered out ("locked out" of the solution). For land, we computed the mean Human Footprint index[14] within recent PAs (≤10 years) in each country and locked out areas with values above 10 or the computed 90th percentile. For national waters, we computed the mean Cumulative Human Impact[15] within recent (≤10 years) PAs in each country, excluding climate-change-related stressors, and locked out areas above the 90th percentile.

Species coverage targets

We determined conservation targets for individual species' ranges, an approach that has been shown to produce superior results to using species richness as a proxy for biodiversity.[16] Hence, following Allan et al.,[17] we obtained data on the distributions of terrestrial mammals (n = 5,272), amphibians (n = 6,352), reptiles (n = 4,379), freshwater crayfish (n = 491), and dragonflies and damselflies (order Odonata; n = 1,104) from the

[10] Also called exclusive economic zones (EEZs).
[11] Amazon Web Services, 512-gigabyte random-access memory.
[12] C. S. Martin et al., "A global map to aid the identification and screening of critical habitat for marine industries," *Marine Policy*, March 2015, Volume 53, pp. 45–53.
[13] G. Dubois et al., Digital Observatory for Protected Areas (v4), Joint Research Center for the European Commission, 2018, www.jrc.ec.europa.eu.
[14] O. Venter et al., "Global terrestrial Human Footprint maps for 1993 and 2009," *Scientific Data,* August 23, 2016, Volume 3. Article Number 16067, pp. 1–10, nature.com.
[15] B. S. Halpern et al., "Recent pace of change in human impact on the world's ocean," *Scientific Reports*, August 12, 2019, Volume 9, Article 11609, pp. 8, nature.com.
[16] V. Veach et al., "Species richness as criterion for global conservation area placement leads to large losses in coverage of *bioRxiv* 839977," *Diversity and Distributions*, April 27, 2017, Volume 23, Number, pp. 715–26, onlinelibrary.wiley.com.
[17] J. R. Allan et al., "Conservation attention necessary across at least 44% of Earth's terrestrial area to safeguard biodiversity," 2019, *bioRxiv,* November 12, 2019.

IUCN Red List of Threatened Species.[18] We complemented these data with range maps for 10,064 reptile species,[19] and bird distribution data (n = 10,926) obtained from IBAT.[20] Furthermore, we obtained data on the distributions of marine mammals (n = 136), sharks, rays, and chimaeras (n = 1,198) as well as marine fish (n = 1,700) from the IUCN Red List of Threatened Species. In addition, to account for the greater migratory behavior of marine animals, we included in the prioritization a global layer of potential and likely critical habitats from Martin et al.,[21] including sea-turtle nesting sites, cold- and warm-water corals, seamounts, seagrass beds, salt marshes, hydrothermal vents, and cold seeps (critical habitats that represent 4 percent of the ocean surface).

Following Allan et al.,[22] we set relative species-protection targets decreasing with increasing range size, starting from 100 percent protection for a range smaller than 1,000 square kilometers and log-linearly decreasing to 10 percent for a range greater than 250,000 square kilometers. We limited the target for species with large ranges to a maximum of 1 million square kilometers. For terrestrial prioritization, we also treated disconnected distribution ranges of a single species as distribution ranges of separate species.

Finally, for marine prioritization, we set a coverage target of 100 percent of critical habitats.

Spatial-units coverage

For reasons outlined in this report, we used the proposed UN Convention on Biological Diversity target to conserve 30 percent of the planet by 2030[23] as a reference point for our analysis. We set conservation coverage targets of 30 percent for each defined subdivision of the Earth that we referred to as spatial units. Depending on the scenario, these spatial units are, respectively, each country, each ecoregion, and each ecozone.

Cost minimization

While meeting the constraints defined by the conservation problem, the algorithm finds a solution for which the sum of the costs of the selected PUs is minimized. Costs in a conservation problem can take various forms, such as acquisition and operating costs, opportunity costs, or sociopolitical value.

To test the sensitivity of the location of areas identified for conservation and related benefit and cost metrics, we ran the algorithm with two different definitions of costs:

1. For terrestrial prioritization, we defined costs as opportunity costs related to the reduction of climate-change-mitigation ecosystem services if they were not conserved—in other words, the higher the ecosystem service value, the lower the cost of conservation. We first collected layers of carbon stocks in above- and below-ground biomass and soils.[24] Then, to place more emphasis on carbon that is at risk of being released in the future, we used projected emissions of CO2 from deforestation in the tropics[25] by 2050 (see section "How we estimated carbon non-emitted from land-use change

[18]The IUCN Red List of Threatened Species data downloaded from the Integrated Biodiversity Assessment Tool (IBAT) (http://www.ibat-alliance.org). Provided by BirdLife International, Conservation International, IUCN, and UNEP-WCMC. Please contact ibat@ibat-alliance.org for further information.

[19]S. Meiri et al., data from U. Roll et al., "The global distribution of tetrapods reveals a need for targeted reptile conservation," Dryad, Data set: U. Roll et al., *Nature Ecology & Evolution*, 2017, Volume 1, pp. 1677–82.

[20]BirdLife International and Handbook of the Birds of the World, bird species distribution maps of the world (version 2018.1), 2018. Obtained from IBAT.

[21]: Martin, C. S. et al. A global map to aid the identification and screening of critical habitat for marine industries. *Marine Policy* 53, 45–53 (2015).

[22]J. R. Allan et al, "Conservation attention necessary across at least 44% of Earth's terrestrial area to safeguard biodiversity." 2019, *bioRxiv* 839977.

[23]Update of the zero draft of the post-2020 global biodiversity framework, UN Convention on Biological Diversity, August 17, 2020, cbd.int.

[24]L. Watson et al., "Global ecosystem service values in climate class change", *Environmental Research Letters,November* 2019, Issue 15, Number 2.

[25]From 2000 to 2010, 139.1 megahectares of tropical land were deforested (Busch et al., 2019), representing 81 percent of global deforestation estimated at 172.5 megahectares over the same period. Data from Global Forest Watch, "Global tree cover loss," accessed September 9, 2020, globalforestwatch.org.

avoidance"), scaled from one to ten and then multiplied by carbon stocks. The result is that carbon stocks "at risk" were given up to ten times the value of carbon stocks with lower risks of emission. We, finally, scaled the resulting layer to a score of 0 to 1 (0 = highest value, 1 = lowest). For marine prioritization, we set costs to be constant and equal to 1 for all PUs, given a lack of sufficiently exhaustive and spatially explicit data for blue carbon stocks and degree of risk to those carbon stocks.

2. Following Allan et al., we set costs to be equal to the HFP index for terrestrial prioritization and the CHP index for marine prioritization. The lower the HFP/CHP index, the lower the impact of conservation on existing human activity.

Selection of 30 percent for conservation

With the given constraints, the solution to the conservation problem might cover more than 30 percent of land and national waters. Hence we assessed the relative importance—also called irreplaceability—of each PU and kept only those with the highest importance under the 30 percent scenario. We considered the importance as the inverse of the costs (the higher the cost, the lower the importance). In the only case where costs were defined to be equal to 1 (marine prioritization), we computed the rarity-weighted richness,[26] which enabled us to select the PUs covering the largest number of species in the fewest number of sites.[27]

Implementation of different prioritization scenarios

We combined the different definitions of spatial-units coverage (n = 3) and costs (n = 2) to form six scenarios for the conservation of 30 percent of land and national waters. This enabled us to explore the impact of the prioritization approach on the benefits and costs of conservation.

Impact metrics linked to the prioritization methodology

Impact metrics were estimated for all PARs and NCAs. The impact of existing PAs (excluding PARs) was not analyzed.

How we estimated species representativeness

We evaluated how much area, on average, of a species range was covered within NCAs and PARs. Using species-range maps,[28] we calculated—split by IUCN Red List category (critically endangered, endangered, vulnerable, near threatened, etc.) —the percentage of the total species range that is covered within each individual existing PA, PAR, and NCA. We then compared the species-range coverage under the current PA network and the projected 30 percent PA network.

How we measured CO_2 abatement potential

Two forms of potential CO_2 abatement were estimated: avoided deforestation in the tropics and reforestation.

How we estimated carbon non-emitted from land-use change avoidance

We relied on Busch et al.[29] to estimate areas that are likely to be deforested and associated CO_2 emissions in the tropics by 2030 and by 2050. The approach of Busch et al. is based on a gridded land-cover change model accounting

[26] Rarity-weighted richness of a PU is the sum for all species of their rarity, defined as the inverse of the number of PUs in which a species occurs. P. Williams et al., "A comparison of richness hotspots, rarity hotspots, and complementary areas for conserving diversity of British birds," *Conservation Biology*, 1996, Volume 10,Number 1, pp. 155–74.

[27] F. Albuquerque and P. Beier, "Rarity-weighted richness: A simple and reliable alternative to integer programming and heuristic algorithms for minimum set and maximum coverage problems in conservation planning," *PLoS ONE*, March 17, 2015, Volume 10, Number 3, journals.plos.org.

[28] The IUCN Red List of Threatened Species data downloaded from the Integrated Biodiversity Assessment Tool (IBAT) (www.ibat-alliance.org). Provided by BirdLife International, Conservation International, IUCN and UNEP-WCMC. Please contact ibat@ibat-alliance.org for further information.

[29] J. Busch et al., "Potential for low-cost carbon dioxide removal through tropical reforestation," *Nature Climate Change*, June 2019, Volume 9, Issue 6, pp. 463–6.

for site characteristics such as slope, elevation, protected status, initial forest cover, and agriculture-revenue potential. We reproduced their results using provided codes and input layers[30] under their Business As Usual (BAU) scenario (that is, no changes in agro-ecological, economic, and policy conditions that affect land-cover change). We found a projected deforested area of 4.93 square megakilometers from 2020 to 2050, corresponding to emissions of approximately 220 gigatonnes of CO_2.[31]

We then overlaid the NCAs and PARs with the map of projected emissions and calculated the total CO_2 emissions projected within them by 2030 and 2050. These emissions can be considered as the maximum CO_2 emissions as if the area were not conserved under a BAU scenario.

Avoiding all deforestation within PAs is probably not feasible,[32] but, since the global extent and geographical distribution of deforestation is imprecise, we assumed 80 percent of these projected emissions could be avoided when areas are conserved, provided that sufficient financial means are dedicated to surveillance and enforcement. This is a fixed haircut, irrespective of a given carbon price that would incentivize or disincentivize the avoidance of deforestation.[33]

Almost doubling PA coverage may potentially induce leakage (that is, displacement of deforestation to other, unprotected areas, either locally or internationally). However, there is also evidence that blockage (that is, a decrease in deforestation surrounding a conservation area) occurs more often than leakage.[34] Until more is known on the relative importance of these effects in different geographies, we have assumed leakage and blockage offset each other.

How we estimated potential carbon stored following reforestation

To estimate the potential carbon stored following reforestation, we started by creating a map of global reforestation potential, following Bastin et al.[35] To do so, we first predicted tree coverage globally under natural conditions, independently of land use. Based on their data set of observed tree coverage within PAs (78,774 photo-interpreted measurements), we trained a Random Forest model[36] using a set of spatial predictors at a resolution of 1 ×1 kilometer grouped in four categories:

1. climate variables:[37]mean annual temperature, mean temperature in the wettest quarter, annual precipitation, precipitation seasonality, and precipitation in the driest quarter

2. topographic variables:[38] slope, elevation, and hill shade

3. soil variables:[39] bedrock depth, sand content, and World Reference Base soil class

[30] J. Engelmann and J. Busch, "Replication data for: Potential for low-cost carbon dioxide removal through tropical reforestation," *Harvard Dataverse*, 2019, V5.
[31] Our figures are slightly lower than those of Busch et al. (5.415 Mkm^2 of deforestation and 256.9 Gt CO_2 emissions from deforestation from 2020 to 2050 under a BAU scenario).
[32] M. Heino et al., "Forest loss in protected areas and intact forest landscapes: A global analysis," *PLoS ONE*, October 14, 2015, Volume 10, Number 10, journals.plos.org.
[33] J. Busch et al., "Potential for low-cost carbon dioxide removal through tropical reforestation," *Nature Climate Change*, June 2019, Volume 9, Issue 6, pp. 463–6.
[34] C. Fuller et al., "First, do no harm: A systematic review of deforestation spillovers from protected areas," *Global Ecology and Conservation*, April 2019, Volume 18, sciencedirect.com.
[35] J.-F. Bastin et al., "The global tree restoration potential," *Science,* July 5, 2019, Volume 365, Number 6448, pp. 76–9.
[36] L. Breiman, "Random forests," *Machine Learning,* October 2001, Volume 45, pp. 5–32.
[37] S. E. Fick and R. J. Hijmans, "WorldClim 2: New 1-km spatial resolution climate surfaces for global land areas," *International Journal of Climatology*, October 2017, Volume 37, Number 12, pp. 4302–15, rmets.onlinelibrary.wiley.com.
[38] Derived from Shuttle Radar Topography Mission (SRTM) 1 Arc-Second Global, US Geological Survey, usgs.gov.
[39] T. Hengl et al., "SoilGrids250m: Global gridded soil information based on machine learning," *PLoS ONE*, February 16, 2017, Volume 12, Number 2, journals.plos.org.

4. biogeographic variables:[40] biome and continent

Hyperparameter tuning was made using R's caret package[41] and repeated cross-validation with 40 folds and setting the number of trees at 500.

After transforming tree cover to forest cover, according to the definition of the Food and Agriculture Organization (FAO) of the United Nations,[42] we calculated the theoretical reforestation potential as the difference between the predicted forest cover and the current forest cover.[43] We then filtered out a range of areas where reforestation is either not likely to happen or has adverse or unclear benefits for climate mitigation or the environment:

1. areas under urban and cropland land cover[44]

2. areas defined as arid and hyperarid[45]

3. boreal forest/taiga; grassland, tropical savanna, and shrubland; and desert and xeric shrubland biomes[46]

We then converted the reforestation potential to biome-specific CO_2-sequestration potential.[47] The resulting reforestation potential covers 4.29 square megakilometers, corresponding to a sequestration potential of 218 gigatonnes of CO_2 if these areas where restored to the status of mature forests.

Finally, we overlaid NCAs and PARs with the reforestation map and calculated the sum of the CO_2-sequestration potential in each area, thereby assuming that 100 percent of the restoration potential will take place. Similarly to deforestation avoidance, this assumes that the NCA will have enough funding to be established and operate after its creation. We further assumed the total sequestration potential would be reached within 100 years following a linear sequestration rate, so that 10 percent of the sequestration potential would be achieved by 2030.

Measuring zoonotic disease risk

To estimate the zoonotic risk covered by NCAs and PARs, we used a global map of the predicted risk of zoonotic emerging infectious disease (EID), provided by Allen et al.[48, 49] The predicted risk tends to be higher in regions experiencing land-use changes and where biodiversity is high. We used the true, unbiased risk index, which factors out measured-reporting efforts and factors in human population (and which corresponds to the observed risk multiplied by human population and divided by the reporting efforts).

[40] D. M. Olson et al., "Terrestrial ecoregions."
[41] M. Kuhn, "Building predictive models in R using the caret package," *Journal of Statistical Software*, November 10, 2008, Volume 28, Number 5, pp. 26, statsoft.org.
[42] Land of at least 0.5 hectares with at least 10 percent tree cover.
[43] Derived from M. Buchhorn et al., "Fractional forest cover layer," 2019, Copernicus Global Land Service: Land Cover 100m: collection 2: epoch 2015, Globe (Version V2.0.2).
[44] Land cover classes 10, 20, and 190, from M. Buchhorn et al., Bruno Smets, Luc Bertels, Myroslava Lesiv, Nandin-Erdene Tsendbazar, Martin Herold, & Steffen Fritz. 2019. Copernicus Global Land Service: Land Cover 100m: collection 2: epoch 2015: Globe (Version V2.0.2).
[45] Derived from A. Trabucco and R. J. Zomer, "Global Aridity Index and Potential Evapotranspiration (ET0),"Climate Database v2. *figshare*. Dataset, 2019.
[46] Following J. W. Veldman et al., "Comment on the global tree restoration potential," *Science*, October 18, 2019, Volume 366, Number 6463, sciencemag.org, we excluded trees planted in boreal forests, tundra, and montane grasslands and shrublands, which can have a negative net warming effect due to a decrease of albedo. Similarly, we excluded savanna and grassland biomes, as tree planting in these regions will likely threaten biodiversity, through habitat replacement and increased fire risk, and reduce food security for locals relying on these biomesfor livestock forage, hunting, or water supply.
[47] J. W. Veldman et al., "Comment on 'The global tree restoration potential',."
[48] T. Allen et al., "Global hotspots and correlates of emerging zoonotic diseases," *Nature Communications*, October 24, 2017Volume 8, Article Number 1124, nature.com.
[49] Generated from R scripts found at Zenodo. (https://zenodo.org/record/400978).

We computed the sum of the risk in five areas: existing PAs, PARs, areas that cannot be protected due to a high level of human activity (locked-out areas—see section "Areas locked in, locked out"), NCAs, and, finally, the remaining areas ("unprotected nature"). We then interpreted the differences in total risk as a reflection of the fact that these areas are carrying a higher or lower risk of EID events, irrespective of their size.

Similarly to the impact of conservation on the risk of species extinction, here we did not quantify the impact of conservation on the reduction of the risk of zoonotic EID. However, empirical evidence suggests that deforestation and land-cover change in high-biodiversity areas are linked to higher EID risks,[50] so protecting nature reduces interactions between humans and other animals and the likelihood of future outbreaks.[51]

Measuring revenue streams and economic impact

Carbon offsets

In line with our quantification of the impact of CO_2, two revenue streams were defined for carbon offsets: deforestation avoidance (carbon credits derived from nonemitted carbon from land-use change), and reforestation.

The 2030 total of equivalent CO_2 stock was discounted to account for the portion of emissions that a country would withhold from voluntary carbon markets to fulfill international country-level emissions targets (in accordance with the Intergovernmental Panel on Climate Change). Based on expert input, an assumed discount of 25 percent was applied. We then annualized the discounted 2030 total CO_2 value in each conservation area, assuming an equal portion each year from 2020 to 2030. Finally, the annual value of potential CO_2 emissions was multiplied by an assumed price for CO_2 offsets: $5 per tonne of CO_2 was deemed moderately to highly conservative, based on expert input, although it should be noted that future supply and demand in the carbon-offset markets remain difficult to forecast.

Terrestrial ecotourism

How we sized total volume and revenue of terrestrial ecotourism

Our analysis of ecotourism revenues was similar to that of Balmford et al.,[52] which estimated the global magnitude of visits to PAs. We extracted visitor data for approximately 500 PAs from Balmford et al., which we individually associated with each corresponding spatial attribute (that is, each polygon) in the WDPA. We excluded records from Chile, because some of them (Cabo de Hornos, for example) indicated they had no visitors, which we considered unlikely to hold true. We replaced these with data from the Corporación Nacional Forestal (CONAF)[53] (n = 75) and further complemented the data set with PA visitor data from Indonesia[54](n = 50), Brazil[55] (n = 28), and South Africa[56] (n = 19).

[50] J. Olivero et al., "Recent loss of closed forests is associated with Ebola virus disease outbreaks," *Scientific Reports*, October 30, 2017, Volume 7, Article Number 14291, nature.com.
[51] J. Olivero et al., "Human activities link fruit bat presence to Ebola virus disease outbreaks," *Mammal Review*, October 30, 2019, Volume 50, Number 1, pp. 1–10, onlinelibrary.wiley.net.
[52] A. Balmford et al., "Walk on the wild side: Estimating the global magnitude of visits to protected areas," *PLoS Biology*, February 24, 2015, Volume 13, Number 2, journals.plos.org.
[53] National Forestry Corporation of Chile, conaf.cl.
[54] Ministry of Environment and Forestry of the Republic of Indonesia, http://perpustakaan.bappenas.go.id/lontar/file?file=digital/161771-[_Konten_]-Konten%20D1185.pdf.
[55] E. Viveiros de Castro, T. Beraldo Souza and B. Thapa, "Determinants of tourism attractiveness in the national parks of Brazil," *Parks,* November 2015, Volume 21, Number 2, parksjournal.com.
[56] South African National Parks Annual Report 2016/2017, sanparks.org.

Using their location, we extracted a set of variables (or a summary of them—for example, minimum, maximum, and average): the continent; remoteness (distance in minutes from the nearest cities with a population of 50,000 to one million[57]), natural attractiveness (count of mammals from the IUCN database of threatened species, considering only species in the categories "vulnerable," "endangered," or "critically endangered"), average country GDP per capita from 2000 to 2007,[58] population density[59] (inside the PA and outside the PA within a 100-kilometer distance), HFP (inside and outside the PA), PA size, average number of country visits from 1997 to 2007 (yearly tourist arrivals[60]), violent crime index in 2008 (qualitative variable based on the likelihood of violent crime threatening government activities in the next two years[61]), the global peace index[62] in 2008, and the variation in elevation (elevation at a 5-kilometer grid resolution was used as a proxy for the presence of mountains[63]).

These variables were used to train a supervised random-forest regression model. All variables, including the dependent variable, were log-transformed. Seventy-five percent of the data were kept for calibration, while the rest were used to validate the model. Hyperparameter tuning was done using R's caret package[64] and repeated cross-validation with 40 folds and setting the number of trees to 500. The resulting model, with an R^2 of 0.6 on the validation set, enabled us to estimate the potential number of visits per year to NCAs and PARs (see Schägner et al.[65] for a similar approach).

While random forest models are flexible and can fit nonlinear, complex problems, extrapolation of the predictions outside the calibration space is likely to fail and hence is not recommended.[66] To mitigate this issue, we first limited predictions of the number of visitors to the range observed in the calibration set by continent (for example, if the number of visitors in Africa ranges from 100 to 100,000 visitors a year, predictions in Africa will be bounded to a minimum of 100 and a maximum of 100,000). Second, because there were no calibration points in countries with low tourism potential due to insecurity or other sociopolitical reasons, we made no predictions for countries with a global peace index lower than that which was observed in the calibration data set.[67]

Finally, we multiplied the predicted number of visits by a monetary-value estimate, according to the unit-value-transfer approach, which is a standard approach in ecosystem service-value mapping. To do so, we used the median revenues per visit (in 2014 US dollars) for each continent, as reported by Balmford et al[68]: Africa, $698/visit; Asia, $85/visit; Oceania, $85/visit ; Europe:, $23/visit; North America, $103/visit; and South America, $311/visit.

The predicted monetary value for each NCA and PAR calculated as we have discussed was a 2003 value in terms of 2014 US dollars. To estimate the 2030 ecotourism value for all conservation areas (existing PAs plus PARs plus NCAs), the predicted 2003 revenues in existing PAs were projected for 2030 using

[57]A. Nelson et al., "A suite of global accessibility indicators," *Scientific Data*, November 7, 2019, Volume 6, Article Number 266, nature.com.
[58]The World Bank, worldbank.org.
[59]Gridded population of the world (version 4), Socioeconomic Data and Applications Center (SEDAC), sedac.ciesin.columbia.edu.
[60]M. Roser, "Tourism," *Our World in Data*, 2017, ourworldindata.org.
[61]"Peace Index 2019: Measuring peace in a complex world,"*Institute for Economics & Peace*, June 2019, visionofhumanity.org.
[62]Ibid.
[63]G. Amatulli et al., "A suite of global, cross-scale topographic variables for environmental and biodiversity modeling," *Scientific Data,* March 20, 2018, Volume 5, Article Number 180040, nature.com.
[64]M. Kuhn, "Building predictive models in R using the caret package."
[65]J. P. Schägner et al., "Mapping recreational visits and values of European National Parks by combining statistical modelling and unit value transfer," *Journal for Nature Conservation*, June 2016, Volume 31, pp. 71–84, sciencedirect.com.
[66]T. Hengl et al., "Global mapping of potential natural vegetation: An assessment of machine learning algorithms for estimating land potential," *PeerJ*, August 22, 2018, Volume 6, peerj.com.
[67]In 2008, the country with the highest global peace index in the calibration dataset (i.e., the worst) had a value of 2.7. Hence, we excluded all the countries with a global peace index above this threshold in 2020. It should be noted that this index represents a simplification and that our exclusion of these countries in our analysis does not imply that they have no ecotourism potential.
[68]Balmford, A., Green, J. M., Anderson, M., Beresford, J., Huang, C., Naidoo, R., ... & Manica, A. (2015). Walk on the wild side: estimating the global magnitude of visits to protected areas. *PLoS Biology*, 13(2), e1002074

a country-specific CAGR of annual overnight arrivals from 2003 to 2029 provided by global Oxford Economics data. If country-level data were unavailable, a regional CAGR weighted by gross overnight visits was applied.

Before taking the forecasted global 2030 ecotourism market value for conservation areas and estimating it for each NCA and PAR, we considered an additional filter to exclude NCAs that would not allow ecotourism—specifically, PAs under IUCN category Ia. Category Ia PAs were identified as those with a human footprint index less than or equal to 3, which scientific research notes is the range for "low disturbance" in an area.[69] Any NCA or PAR at or below this threshold was given a value of zero visitors projected for 2030.

Finally, we distributed the 2030 ecotourism market value for conservation areas, calculated as we have described, to existing PAs, PARs, and NCAs, prorated by the estimated number of visitors to each area as a portion of a country's predicted total number of visitors to conservation areas.

How we sized the total GDP and jobs created or safeguarded

After sizing the annual revenue value of ecotourism, we used revenue-to-GDP or revenue-to-job multipliers from Oxford Economics data to estimate both GDP and jobs created by or safeguarded from this revenue stream. A country-specific 2019 tourist spending-to-GDP multiplier provided by global Oxford Economics data was applied to the revenue projection for each NCA and PAR. If country-level data were unavailable, we applied a regional multiplier weighted by total-tourist spend. Similarly, for jobs, we applied a country-specific 2019 tourist-spend-to-total jobs multiplier provided by global Oxford Economics data to each NCA and PAR. If country-level data were unavailable, we applied a regional multiplier weighted by total jobs.

Sustainable fishing

How we sized total sustainable fishing revenue

We defined fishing revenue for each NCA and PAR as the value of fish caught at sustainable levels within the Marine Protected Area (MPA), excluding a no-take zone, for areas currently identified as overfished. This assumes that revenues from overfished stocks are likely to collapse in the midterm or long term and that hence protecting these areas would result in net benefits in the same time horizon.

First, we collected global historical industrial and nonindustrial catches from 1950 to 2015 at 0.5-degree resolution from Sea Around Us[70] and kept only those under "reported" and "illegal, unreported, and unregulated (IUU)" fishing. We then assigned catch data to each of the 19 corresponding UN Food and Agriculture Organization (FAO) fishing areas. We considered the combination of a species taxon and FAO area as a separate stock, following the approach used by the Ocean Health Index.[71] Each taxon was assigned a resilience[72] level (low, medium, or high) sourced from the Ocean Health Index website.[73] We then used catch data and resilience to estimate the biomass available and the maximum sustainable yield

[69] K. Mokany et al., "Reconciling global priorities for conserving biodiversity habitat," *PNAS*, May 5, 2020, Volume 117, Number 8, pp. 9906–11, pnas.org.
[70] R. A. Watson and A. Tidd, "Mapping nearly a century and a half of global marine fishing: 1869–2015," *Marine Policy*, July 2018, Volume 93, pp. 171–7.
[71] "Fisheries: Status," *Ocean Health Index*.
[72] The ecological resilience is the capacity of an ecosystem to recover after disturbance.
[73] "Fisheries: Status," Ocean Health Index, oceanhealthindex.org.

(MSY)[74] per stock with a catch-only MSY (CMSY) model, following Martell and Froese[75]as implemented in the *datalimited* R package,[76] keeping all stocks that have an average annual harvest of at least 1,000 tonnes and with a time series of at least 20 years. Using CMSY, we also computed B/BMSY,[77] a proxy for stock status, with a value less than 1 indicating overfishing. We then removed stocks that are underfished or fully exploited, which we defined as those with a B/BMSY greater than 0.95, to account for uncertainties in the CMSY outputs.

For the remaining stocks, we computed the ratio of catch for a given stock within the MPA to the total catch within the FAO region—which, in other words, corresponds to a "market share" per stock per MPA. In calculating the market share, we excluded catches captured by bottom trawling gears, to avoid accounting within NCAs and PARs for fishing practices that are destructive to ocean habitats.

We defined each stock MSY level as the target catch allowed within an MPA and multiplied this value by its market share. We further haircut by 30 percent the target catch, effectively creating a marine no-take zone of 30 percent of the MPA's surface. For the purpose of sustaining fishing, most studies recommend setting 20 to 40 percent of fishing grounds aside as no-take areas.[78] We postulated here that creating MPAs with no-take areas allows regulated fishing to balance the trade-off between biodiversity conservation and fishing output[79] Considering that a recent empirical study[80] showed that closing fishing in two of the largest MPAs on Earth had a minimal impact on the economics of the fishing industry, the application of this haircut results in a conservative estimate of the value of MPAs.

Finally, we multiplied the yearly target catch within MPAs by their average stock value during the period from 2006 to 2016 using a database of ex-vessel fish prices,[81] which we summed to get the total revenues from sustainable fishing in new MPAs.

How we sized the total GDP and jobs created or safeguarded

After sizing the annual revenue value of sustainable fishing, we aimed to estimate both GDP and jobs created or safeguarded from this revenue stream using revenue-to-GDP or revenue-to-job multipliers from World Input-Output data.[82] We used GDP and jobs data from 51 countries to estimate country-specific or regional 2014 revenue-to-total GDP and revenue-to-total job multipliers. If country-level data were unavailable, we applied a regional multiplier weighted by GDP or jobs, respectively.

Marine ecotourism

Marine ecotourism can be defined as nature-based tourism that is directly dependent on preserved marine ecosystems. Our analysis of marine ecotourism revenues was based on two main revenue streams: coral reef tourism (which includes snorkeling, scuba diving, glass-bottom-boat tours, and underwater photography); and marine-life-observation tourism. In both cases, we estimated the revenue based on

[74] Maximum sustainable yield is a term used in fishery management to describe the highest average catch (by weight) that does not reduce a stock's abundance over time, taking into account the stock's reproductive and growth capacities under prevailing environmental conditions.
[75] S. Martell and R. Froese, "A simple method for estimating MSY from catch and resilience," Fish and Fisheries, December 2013, Volume 14, Number 4, pp. 504–14, onlinelibrary.wiley.com.
[76] Stock assessment methods for data-limited fisheries, datalimited, https://github.com/datalimited/datalimited.
[77] B stands for "biomass," and BMSY is the biomass that enables a fish stock to deliver the maximum sustainable yield.
[78] L. Pet-Soede et al.,"Benefits of marine protected networks: An overview in support of the Coral Triangle Initiative," *World Wildlife Fund*, June 2009.
[79] F. Vandeperre et al., "Effects of no-take area size and age of marine protected areas on fisheries yields: A meta-analytical approach," *Fish and Fisheries*, December 2010, Volume 12, Number 4, pp. 412–26, onlinelibrary.wiley.com.
[80] J. Lynham et al., "Impact of two of the world's largest protected areas on longline fishery catch rates," *Nature Communications*, February 20, 2020, Volume 11, Article Number 979, nature.com.
[81] T. C. Tai et al., "Ex-vessel fish price database: Disaggregating prices for low-priced species from reduction fisheries," *Frontiers in Marine Science*, November 13, 2017, Volume 4, Article Number 363, frontiersin.org.
[82] The World Input-Output Database, wiod.org.

our derivation of a value per square kilometer resulting from the defined tourist-related activities (in US dollars per square kilometer), which we multiplied by the areas of the NCAs and PARs (according to the unit value transfer approach).

How we sized total reef tourism revenue

The reef ecotourism revenue from MPAs was calculated using data from Spalding et al. Spalding et al.[83] gathered data about coral-reef ecotourism for 80 countries and derived the average value of total reef area per country (expressed in 2013 US dollars per square kilometer). To obtain the value of reef tourism for each NCA and PAR, we used a global database of coral-reef locations[84] to compute the surface covered by coral reefs and multiplied it by its value per area unit.

How we sized total marine mammals and shark watching revenue

Data on revenues associated with marine mammals and shark ecotourism from PAs were obtained from O'Connor et al.,[85] who reported country whale-watching-industry data in 1998 and 2008 gathered via surveys (by, for example, whale-watching operators, government tourism offices, academics, and researchers) and through an in-depth literature review. Whale watching was defined to cover the viewing of all cetacean species, including whales, dolphins, and porpoises (but not whale sharks or basking sharks). Available data points include:

— the number of whale watchers per country in 1998 and 2008

— growth, based on the evolution of the number of whale watchers

— direct expenditure—for example, the purchase price paid by participants to engage in the whale-watching activity, in 2009 US dollars

— indirect expenditure—for example, the expenditure into the local economy that can be attributed to a person participating in the whale-watching activity in addition to the direct expenditure on the ticket, in 2009 US dollars

To account for the trend in whale-watching activities until 2030, we used growth rates reported by O'Connor et al. to project 2008-to-2030 values.

In addition, to include revenues linked to other species such as sharks, rays, and chimaeras, we collected data from Cisneros-Montemayor et al.,[86] who provided shark-watching and game-fishing expenditures (in US dollars per year in 2011) for 20 countries. For consistency, the expenditures were converted to 2009 US dollar values. We assumed no overlap with the revenues calculated for coral reef-associated tourism, given the lack of reliable data that would enable discrimination between these two activities.

[83] M. D. Spalding et al., "Mapping the global value and distribution of coral reef tourism," *Marine Policy*, August 2017, Volume 82, pp. 104–13, sciencedirect.com.

[84] M. D. Spalding, R. D. Brumbaugh and E. Landis, *Atlas of Ocean Wealth*, Arlington, Virginia: The Nature Conservancy, 2016. UNEP-WCMC, WorldFish Centre, WRI, TNC (2018). Global distribution of warm-water coral reefs, compiled from multiple sources including the Millennium Coral Reef Mapping Project. Version 4.0. Includes contributions from IMaRS-USF and IRD (2005), IMaRS-USF (2005) and Spalding et al. (2001). Cambridge (UK): UN Environment World Conservation Monitoring Centre. URL: http://data.unep-wcmc.org/datasets/1

[85] S. O'Connor et al., "Whale watching worldwide: Tourism numbers, expenditures and expanding economic benefits. A special report from the International Fund for Animal Welfare," 2009.

[86] A. M. Cisneros-Montemayor et al., "Global economic value of shark ecotourism: Implications for conservation," *Oryx*, July 2013, Volume 47, Number 3, pp. 381–8, cambridge.org.

Bird- and pinniped-watching activities were not included in our analyses because they are observed mostly from land and were therefore considered part of the terrestrial-ecotourism assessment.

To estimate the revenues from marine-mammal and shark-watching ecotourism, we first created a 50-kilometer buffer zone around coasts globally. This zone represented offshore areas in which these activities are likely to take place, as we considered the marine-mammal- and shark-watching boats likely to operate mostly within a 50-kilometer range from coasts. We then intersected the offshore area and countries' exclusive economic zones (EEZs) to compute the exploitable surface for marine-mammal- and shark-watching activities for each country and divided the total annual expenditure per country by this exploitable area to obtain a value in dollars per square kilometer, similarly to how Spalding et al. obtained a reef value per country. We finally calculated the intersection of each NCA and PAR with the exploitable area and multiplied the resulting intersection by the value per unit area, resulting in an estimation related to marine-mammal- and shark-watching activities for each NCA and PAR.

How we sized the total GDP and jobs protected or generated

We took the same approach to sizing marine ecotourism that we did for terrestrial ecotourism. See the "Terrestrial ecotourism" section for details.

Jobs created by conservation-area-management activities

Jobs created by the establishment or enhancement of conservation areas include enforcement, maintenance, and general management occupations. We estimated the quantities of these jobs by deriving a country-specific spend-per-employee multiplier, which yields total jobs for each conservation area when multiplied by the costs of management of the conservation area. This multiplier was estimated using 18 data points of organizational spend and employee numbers from publicly available conservation-department information across multiple countries, for marine and terrestrial areas. This data was used to calculate a spend-per-employee multiplier. We then plotted the relationship between this multiplier and the country's GDP per capita, which yielded a strongly correlated result (spend = 4715 + 3.69 GDP per capita; $R^2 = 0.82$).

Using this linear equation, we estimated spend-per-employee multipliers for all countries with per capita GDP data from the World Bank. The country-specific multipliers were then applied to expected country NCA and PAR costs. If country data were unavailable, we applied a regional multiplier weighted by per-capita GDP.

Conservation-area-management cost

We assessed the operational costs of terrestrial and marine conservation using published equations[87] that show decreasing costs per unit area in larger areas, which is a reflection of economies of scale:[88]

1. *Terrestrial protected-area cost,* $\log_{10}$ USD/(km^2 x year) = 1.61 + 0.57 × GNP per unit area, $\log_{10}$ USD / (km^2 x year) – 0.7 × PPP, $\log_{10}$ – 0.46 × area, $\log_{10}$ km^2

2. *Marine protected-area cost,* $\log_{10}$ USD/(km^2 x year) = 5.02 – 0.80 × area, $\log_{10}$ km^2

[87] USD = US dollars.

[88] A. Balmford et al., "Global variation in terrestrial conservation costs, conservation benefits, and unmet conservation needs," PNAS, February 4, 2003, Volume 100, Number 3, pp. 1046–50, *PNAS*.org

We used for these equations country purchasing power parity (PPP) and gross national product (GNP) values from the World Bank's World Development Indicators. Both equations predict costs per unit area in 2000 US dollars. However, since we used the latest PPP and GNP values for 2018, we assumed terrestrial costs in the first equation to be representative of the year 2018 rather than 2000.

Conversion of all values to present US dollars

In each nature-dependent market, we calculated revenue in different US-dollar monetary values based on when the data were created. Before using revenues to estimate GDP or jobs, we converted all currency to 2020 US dollars using current estimates of inflation. The following nature-dependent markets required conversion:

— terrestrial ecotourism: converted from 2014 US dollars

— sustainable fishing: converted from 2005 US dollars

— marine ecotourism: converted from 2005 US dollars (reef) and 2009 US dollars (whale watching)

Costs were converted to 2020 US dollars using the same approach: terrestrial conservation costs were converted from 2018 US dollars, and marine conservation costs were converted from 2000 US dollars to 2020 US dollars.